Experimental and Theoretical Evidence of a Persistent Radical-Cation Dimer Generated during the Electrooxidation of an N-Glucosamine-pyrrole Derivative

ARTICLE *in* THE JOURNAL OF ORGANIC CHEMISTRY · OCTOBER 2010

Impact Factor: 4.72 · DOI: 10.1021/jo101288j · Source: PubMed

4 AUTHORS:

Ulises Paramo

Instituto Tecnológico de Ciudad Madero, (IT…

18 PUBLICATIONS **65** CITATIONS

SEE PROFILE

Bernardo A. Frontana-Uribe

Universidad Nacional Autónoma de México

64 PUBLICATIONS **849** CITATIONS

SEE PROFILE

Patricia Guadarrama

Universidad Nacional Autónoma de México

61 PUBLICATIONS **327** CITATIONS

SEE PROFILE

Víctor Manuel Ugalde-Saldívar

Universidad Nacional Autónoma de México

40 PUBLICATIONS **348** CITATIONS

SEE PROFILE

JOC Article
pubs.acs.org/joc

Experimental and Theoretical Evidence of a Persistent Radical-Cation Dimer Generated during the Electrooxidation of an *N*-Glucosamine-pyrrole Derivative

Ulises Páramo-García,[†] Bernardo A. Frontana-Uribe,*[,‖,⊥] Patricia Guadarrama,[§] and Victor M. Ugalde-Saldívar[‡]

[†]*Instituto de Química,* [‡]*Facultad de Química, and* [§]*Instituto de Investigaciones en Materiales, Universidad Nacional Autónoma de México, Circuito Exterior, C.U. Coyoacan, D.F. 04510, Mexico, and* [‖]*Centro Conjunto de Investigación en Química Sustentable UAEM-UNAM, Carretera Toluca-Ixtlahuaca Km. 14.5, C.P. 50200, Toluca, Estado de México, México.* [⊥]*Permanent position at the Intituto de Química, Universidad Nacional Autónoma de México, Circuito Exterior, C.U. Coyoacán, D.F. 04510, Mexico.*

bafrontu@servidor.unam.mx

Received July 27, 2010

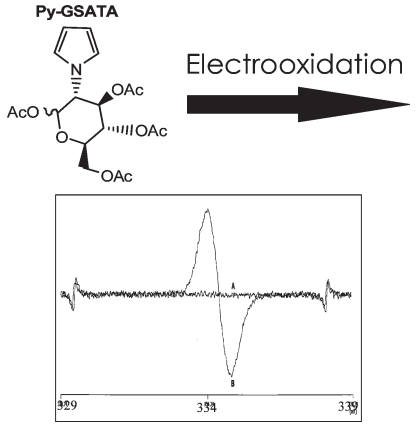

The results of the electrochemical characterization by cyclic voltammetry of 1,3,4,6-tetra-*O*-acetyl-2-amino-2-deoxy-2-(pyrro-1-yl)-*β*-D-glucopyranose (Py-GSATA) are presented. This compound was analyzed in acetonitrile containing 0.1 M tetrabutylammonium perchlorate, using a platinum disk electrode as the working electrode. Py-GSATA showed two irreversible oxidation signals, the first at 1.24 and the second at 1.54 V vs Fc^+/Fc. After successive cyclic voltammetry, under different experimental conditions, it was shown that it is not possible to electropolymerize this pyrrole derivative. Surprisingly, the bulk anodic electrolysis of Py-GSATA generated a single electroactive soluble product with an electrochemical cathodic signal located at −0.35 V vs Fc^+/Fc. Mass spectrometry of the solution showed the presence of a dimeric species of the parent compound. ESR spectroscopy of the electrolysis solution showed a persistent radical species stable at least for 6 months (4 °C). UV−vis spectroscopy was consistent with low chain cation-radical oligomers. In order to propose an explanation to the dimer cation stability in solution, molecular modeling using a B3LYP/6-31+G** level of theory was used to analyze the stability and feasibility of the electrogenerated species.

Introduction

The electropolymerization mechanisms of conducting polymers are a controversial subject; thus, several mechanisms have been proposed to date.[1] One of the most accepted[2] involves *σ*-dimers, which are dicationic products of a fast radical-cation coupling as intermediates of the process.[3] Despite the double charge of the species involved, experimental

(1) (a) Vernitskaya, T. V.; Efimov, O. N. *Russ. Chem. Rev.* **1997**, *66*, 443–457. (b) Sadki, S.; Schottland, P.; Brodie, N.; Sabourand, G. *Chem. Soc. Rev.* **2000**, *29*, 283–293.

DOI: 10.1021/jo101288j Published on Web 10/14/2010

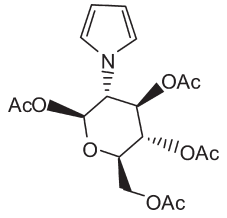

FIGURE 1. 1,3,4,6-Tetra-*O*-acetyl-2-(pyrro-1-yl)-2-deoxy-*β*-D-glucopyranose (**1**, Py-GSATA).

and theoretical investigations support this proposal.[4] The stability of radical cations is a key factor during electropolymerization. Extremely reactive radical cations combine with solvent or other nucleophiles close to the electrode surface, inhibiting polymerization. More stable radical cations diffuse away from the electrode surface, resulting in the formation of soluble oligomers. Only radical cations with moderate stability enhance radical−radical coupling, thus favoring the conducting polymer film formation. Radical-cation stability is enhanced by a high resonance of the unpaired electron[5] and steric hindrance of the site where the radical is located;[6] both effects can be cooperative favoring the radical-cation lifetime. End-capped radical-cation oligomers show good stability due to the blockage of the positions where the polymerization takes place.[7,8]

The oligomerization−polymerization process has been studied by different techniques, and each one gives valuable information on the involved intermediates. Mass spectrometry of the electrolyzed solution using a rotating disk electrode has been used to determine the size of the soluble oligomers formed during the electropolymerization of pyrroles,[9] UV−vis spectroscopy gives information on the electronic transitions of monomeric and charged species,[10,11] and electron spin resonance (ESR) allows characterization of radical intermediates.[10−13] Molecular modeling and theoretical calculations[14] of the intermediates gives us a clear idea about the favored positions and energy involved in the process.

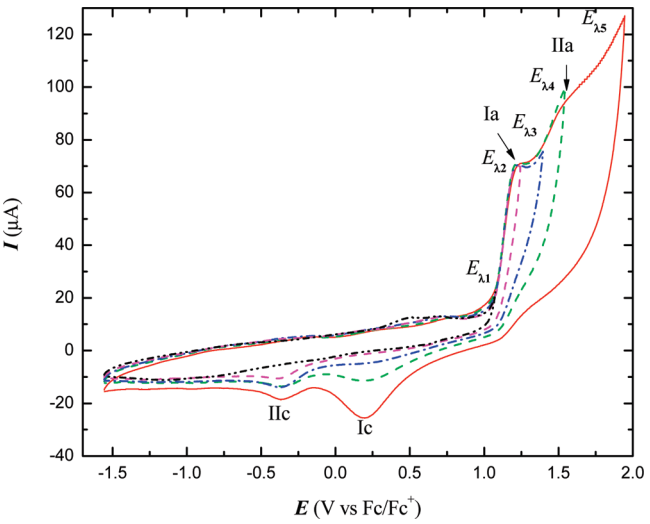

FIGURE 2. Cyclic voltammograms of Py-GSATA (1 mM) in ACN and 0.1 M TBAP at different inversion potential values: WE = Pt, v = 1000 mV/s. $E_{\lambda 1}$ = 1.07 V, $E_{\lambda 2}$ = 1.24 V, $E_{\lambda 3}$ = 1.39 V, $E_{\lambda 4}$ = 1.54 V, and $E_{\lambda 5}$ = 1.94 V.

Interested in the electrosynthesis of chiral conducting polymers, we studied the electrochemical response of 1,3,4,6-tetra-*O*-acetyl-2-amino-2-deoxy-2-(pyrro-1-yl)-*β*-D-glucopyranose (**1**) (Py-GSATA, Figure 1).[15] This compound showed clear oxidation processes that corresponded to the pyrrole oxidation. Nevertheless, the product of the electrooxidation was not the conducting polymer but a stable radical in solution. This paramagnetic species was characterized by cyclic voltammetry, mass spectrometry, and spectroelectrochemical techniques. A theoretical study of the oligomerization process allowed us to understand the oxidation mechanism.

Results and Discussion

Cyclic Voltammetry of Py-GSATA in 0.1 M TBAP−ACN Medium. Figure 2 shows a typical cyclic voltammogram of Py-GSATA obtained in acetonitrile (ACN) and 0.1 M tetrabutylammonium perchlorate (TBAP) using a Pt disk electrode. Two anodic signals were observed at a potential value of 1.24 (Ia) and 1.54 (IIa) V. The first anodic signal was assigned to the irreversible oxidation of the pyrrole group

(2) (a) Heinze, J.; Frontana-Uribe, B. A.; Ludwigs, S. *Chem. Rev.* **2010**, *110*, 4724–4771. (b) Heinze, J. In *Encyclopedia of Electrochemistry*; Bard, A. J., Stratmann, M., Eds.; Wiley-VCH: Weinheim, Germany, 2004; Vol. 8, Chapter 16, pp 607−638. (c) Guyard, L.; Hapiot, P.; Neta, P. *J. Phys. Chem. B* **1997**, *101*, 5698–5706.
(3) Audebert, P.; Hapiot, P. *Synth. Met.* **1995**, *75*, 95–102.
(4) (a) Audebert, P.; Catel, J.-M.; Le Coustumer, G.; Duchenet, V.; Hapiot, P. *J. Phys. Chem. B* **1998**, *102*, 8661–8669. (b) Heinze, J.; John, H.; Dietrich, M.; Tschuncky, P. *Synth. Met.* **2001**, *119*, 49–52. (c) Effenberger, F.; Stohrer, W. D.; Mack, K. E.; Reisinger, F.; Seufert, W.; Kramer, H. E. A.; Foll, R.; Vogelmann, E. *J. Am. Chem. Soc.* **1990**, *112*, 4849–4857.
(5) (a) Odom, S. A.; Lancaster, K.; Beverina, L.; Lefler, K. M.; Thompson, N. J.; Coropceanu, V.; Brédas, J.-L.; Marder, S. R.; Barlow, S. *Chem.—Eur. J.* **2007**, *13*, 9637–9646. (b) Banerjee, M.; Vyas, V. S.; Lindeman, S. V.; Rathore, R. *Chem. Commun.* **2008**, 1889–1891.
(6) (a) Eelkema, R.; Maeda, K.; Odell, B.; Anderson, H. L. *J. Am. Chem. Soc.* **2007**, *129*, 12384–12385. (b) Yoshizawa, M.; Kumazawa, K.; Fujita, M. *J. Am. Chem. Soc.* **2005**, *127*, 13456–13457.
(7) Banerjee, M.; Lindeman, S. V.; Rathore, R. *J. Am. Chem. Soc.* **2007**, *129*, 8070–8071.
(8) Heinze, J.; Tschuncky, P. In *Electronic Materials: The Oligomer Approach*; Müllen, K., Wegner, G., Eds.; Wiley-VCH: Germany, 1998; pp 493−496.
(9) Fermín, D. J.; Scharifker, B. R. *J. Electroanal. Chem.* **1993**, *357*, 273–287.
(10) (a) Van Haare, J. A. E. H.; Groenendaal, L.; Havinga, E. E.; Meijer, E. W.; Janssen, R. A. *J. Synth. Met.* **1997**, *85*, 1091–1092. (b) Heinze, J.; Willmann, C.; Bauerle, P. *Angew. Chem., Int. Ed.* **2001**, *40*, 2861–2864.
(11) (a) Rapta, P.; Neudeck, A.; Petr, A.; Dunsch, L. *J. Chem. Soc. Faraday Trans.* **1998**, *94*, 3625–3630. (b) Rapta, P.; Schulte, N.; Schlüter, A. D.; Dunsch, L. *Chem.—Eur. J.* **2006**, *12*, 3103–3113.
(12) Davies, A. G.; Julia, L.; Yazdi, S. N. *J. Chem. Soc., Perkin Trans. 2* **1989**, 239–244.
(13) Domingo, V. M.; Brillas, E.; Alemán, C.; Julia, L. *J. Chem. Soc., Perkin Trans. 2* **2000**, 905–906.
(14) (a) Waltman, R. J.; Bargon, J. *Tetrahedron* **1984**, *40*, 3963–3970. (b) Beljonne, D.; Brédas, J. L. *Phys. Rev. B* **1994**, *50*, 2841–2849. (c) Lacroix, J.-C.; Maurel, F.; Lacaze, P.-C. *Synth. Met.* **1999**, *101*, 675–676.
(15) Frontana-Uribe, B. A.; Escárcega-Bobadilla, M. V.; Juárez-Lagunas, J.; Toscano, R. A.; García de la Mora, G. A.; Salmón, M. *Synthesis* **2009**, *6*, 980–984.
(16) Gritzner, G.; Küta *Pure Appl. Chem.* **1984**, *56*, 461–466.
(17) (a) Tannor, D. J.; Marten, B.; Murphy, R.; Friesner, R. A.; Sitkoff, D.; Nicholls, A.; Ringnalda, M.; Goddard, W. A., III; Honig, B. *J. Am. Chem. Soc.* **1994**, *116*, 11875–11882. (b) Marten, B.; Kim, K.; Cortis, C.; Friesner, R. A.; Murphy, R. B.; Ringnalda, M. N.; Sitkoff, D.; Honig, B. *J. Phys. Chem.* **1996**, *100*, 11775–11788.
(18) (a) Becke, A. D. *Phys. Rev. A* **1988**, *38*, 3098–3100. (b) Lee, C.; Yang, W.; Parr, R. G. *Phys. Rev. B* **1988**, *37*, 785–789. Implemented as described in (c) Miehlich, B.; Savin, A.; Stoll, H.; Preuss, H. *Chem. Phys. Lett.* **1989**, *157*, 200–206.
(19) Rauhut, G.; Pulay, P. *J. Phys. Chem.* **1995**, *99*, 3093–3100.

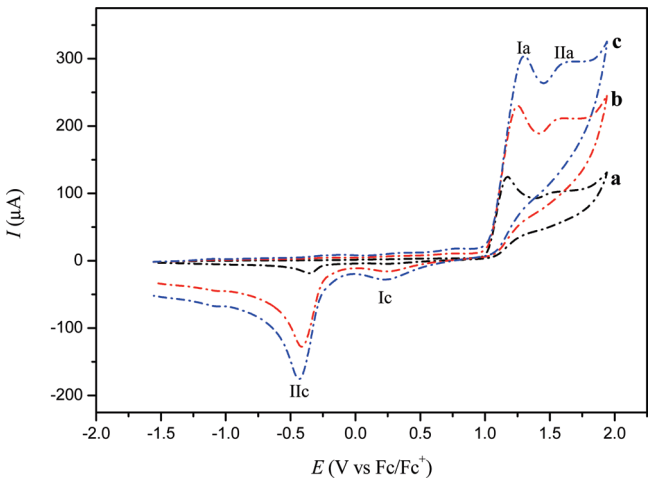

FIGURE 3. Cyclic voltammograms at different scan rates of 10 mM Py-GSATA in ACN and 0.1 M TBAP, using a Pt electrode: (a) 100, (b) 500, and (c) 1000 mV/s.

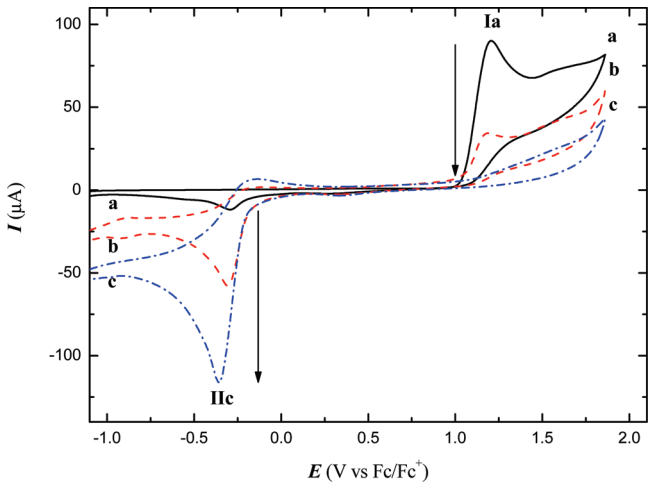

FIGURE 4. Cyclic voltammetry survey of the Py-GSATA (20 mM) electrolysis at 1.35 V vs Fc/Fc^+ in ACN and 0.1 M TBAP, using Pt electrodes in a divided cell: (a) 0, (b) 1.15, and (c) 2.3 F/mol.

and is related, through the reverse scan, to peak IIc located at −0.35 V. This oxidation is located at an unusual high anodic value, compared with pyrroles bearing at the N atom slightly steric hindered groups.[20] This behavior was attributed to a large steric hindrance provoked by the glucosamine rest. The second anodic signal is small and not well-defined. It could be a result of the oxidation of a product at low concentration obtained at the first anodic peak. In the reverse scan a new cathodic signal at 0.20 V (Ic) as consequence of peak IIa appeared. An inversion potential (E_λ) experiment showed that the intensity of both cathodic signals is dependent on this parameter. These cathodic signals could be associated to short chain pyrrole oligomers obtained during the Py-GSATA oxidation.[21] Particularly for peak Ic, its extremely low reduction value fits well with the expected value for a σ-dimer intermediate. These species have been only observed in systems where the pyrrole polymerization reaction is hampered by sterical or electronic factors.[22]

The voltammetric study at different scan rates in the anodic direction showed that the signal size of peak IIa is dependent on the scan rate (Figure S1 in Supporting Information), which is consistent with the previous proposal, and corresponds to the oxidation of an unstable intermediate electrogenerated at the first peak. Thus, peak IIa is better defined at high scan rates, a time scale at which the intermediate generating this peak is easily detected. As the scan rate increases at low concentrations (1 mM), the cathodic signals are more defined and at higher scan rates signal Ic is more important. The cathodic peaks intensity is also dependent on the E_λ value (Figure 2); therefore, if the scan rate study is carried out at the potential value of peak Ia, its current value is proportional to the square root of the scan rate and the favored cathodic signal is peak IIc. If the concentration of the Py-GSATA is increased to 10 mM the voltammetric study at different scan rates (Figure 3) also showed that the signal size of peak IIa is dependent on the scan rate, but the trend of the cathodic peaks inverts, showing always peak IIc as the most intense at all scan rates. From these results, it can be proposed that the classical σ-dimer intermediate (peak Ic) is favored only at low concentrations and fast scan rates and can give rise rapidly to another more stable species that corresponds to peak IIc (*vide infra*).

In order to explore the possibility of electropolymerization of this pyrrole, 30 successive cycles were carried out using the previous experimental conditions (Figure S2 in Supporting Information). The typical increasing current corresponding to the growth of a conductive polymer film[2a] was not observed. Nevertheless, the signal correspondent to peak IIc increases during the cycling. This is an indication of accumulation of an electroactive species at the electrode interface. When the electrode is analyzed in a monomer-free electrolyte solution, it is confirmed that this signal corresponds to a product that is not attached to the electrode but is stable in the electrode interface. The change of solvent (DMF, MeOH, EtOH, and DMSO), electrolytes (tetrabutylammonium tetrafluoroborate, lithium perchlorate, and tetrabutylammonium hexafluorophosphate), and other experimental conditions (lower temperature, different inversion potential values, higher concentrations, and stirring of the solution) did not favor the electropolymerization of Py-GSATA. With the purpose of studying the properties of this electrogenerated stable product detected at peak IIc, preparative scale electrolysis was carried out.

Preparative Scale Electrolysis. To generate the product responsible for peak IIc, the preparative electrolysis of Py-GSATA was carried out inside a double-compartment divided cell. The electrooxidation was performed using 1.35 V vs Fc/Fc^+, a value that corresponds to a potential just after the peak Ia. The cyclic voltammetry survey of the electrolysis is depicted in Figure 4.

It can be observed that the product correspondent to peak IIc accumulates as the electrolysis occurs, but there is no signal of the product correspondent to peak Ic. At the end of the electrolysis there is only one cathodic signal present in the

(20) Diaz, A. F.; Bargon, J. In *Handbook of Conducting Polymers*; Skotheim, TA, Ed.; Marcel Dekker Inc.: New York, 1986; pp 81−115.
(21) (a) Waltman, R. J.; Bargon, J. *Tetrahedron* **1984**, *40*, 3963–3970. (b) Heinze, J.; Willmann, C.; Bauerle, P. *Angew. Chem., Int. Ed.* **2001**, *40*, 2861–2864. (c) Effenberger, F.; Stohrer, W. D.; Mack, K. E.; Reisinger, F.; Seufert, W.; Kramer, H. E. A.; Foll, R.; Vogelmann, E. *J. Am. Chem. Soc.* **1990**, *123*, 4849–4857.
(22) Heinze, J.; John, H.; Dietrich, M.; Tschuncky, P. *Synth. Met.* **2001**, *119*, 49–52.

SCHEME 1. Thermochemical Analysis in Solution (ACN) of the Dimerization Process

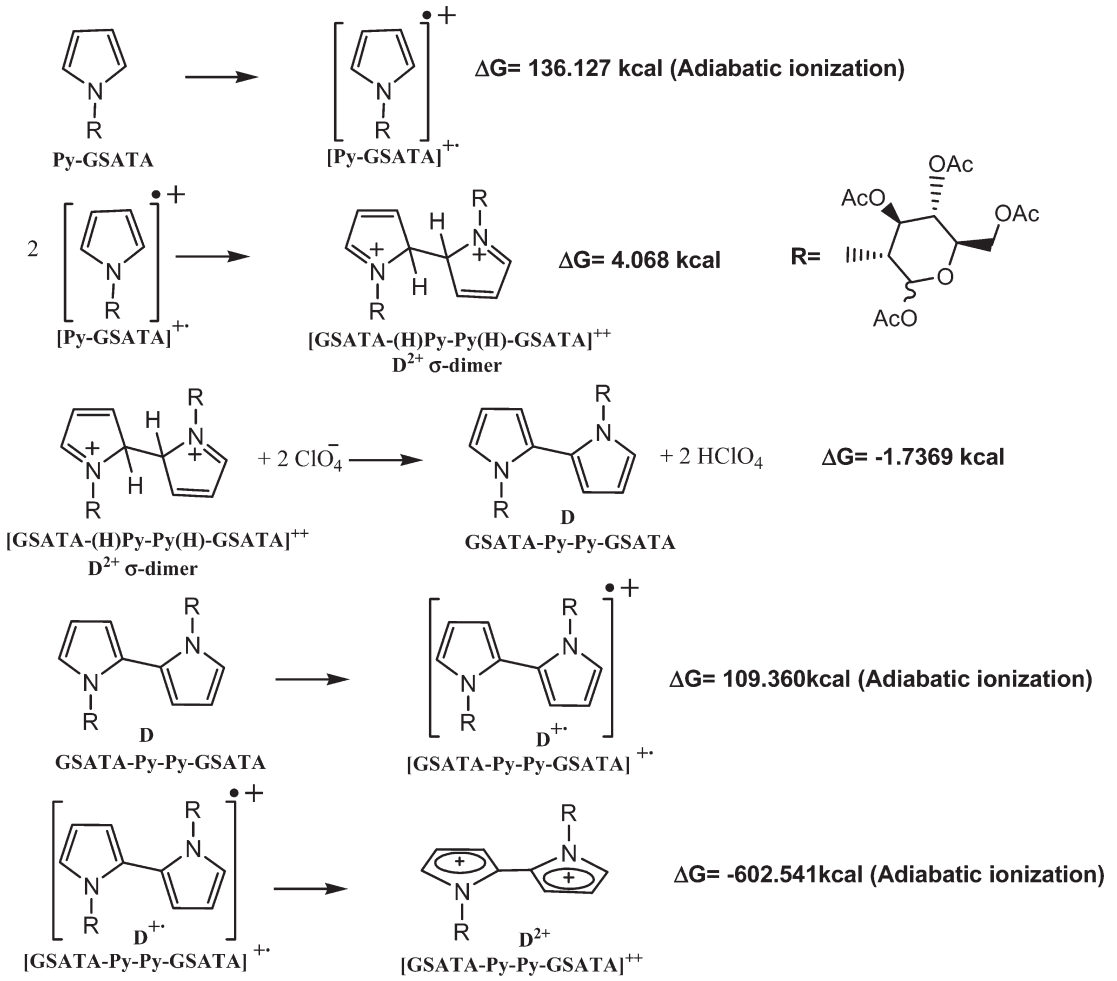

voltammogram with some signs of reversibility (Figure 4, line c). If the electrolysis was carried out at higher anodic potential values (e.g., 1.7 V), the same behavior was observed with almost the same charge consumption and the signal correspondent to peak Ic was never detected at the end of the electrolysis. The charge average of five electrolyses was about 2.1 ± 0.2 F/mol. Thin layer chromatography survey of the electrolysis showed that the starting material was totally consumed, and the major compound obtained was a dark very polar species that did not leave the application point. Attempts to isolate the generated products by selective crystallization or column chromatography were unsuccessful. The products remained attached to the silica gel packing, and it was not possible to elute the compounds. This is an additional indication of a very polar product, for example, an organic salt. If the separation is attempted by ion-pair chromatography, a dark tar composed by a mixture of compounds was obtained. Probably, a disproportionation reaction occurs in the absence of the high polar media generated by the supporting electrolyte. One argument that supports this proposal is the extremely negative ΔG value (ΔG = −602.541 kcal) calculated theoretically for the oxidation of the dimer cation-radical specie during the thermochemical analysis in solution (ACN) (Scheme 1, final reaction). In a second step and fixing the electrolysis potential at −0.5 V, the charge consumed to totally reduce the species that generates peak IIc requiring 1.1 ± 0.2 F/mol was determined. The mass spectroscopy analysis of the electrolysis solution after oxidation at 1.35 V (Figure S3 in Supporting Information) enabled us to identify a dimer with a molecular weight of M = 792. The $[M + 1]^+$ signal generally observed in FAB^+ technique for the expected mass is less abundant than the $[M]^+$; this is an indication that the observed compound has a positive charge. The base peak 242, which corresponds to the electrolyte component tetrabutylammonium cation, confirms this behavior. Following the classical oligomerization route, we propose the presence of the dimer ((2,2′)-GSATA-Py-Py-GSATA) positively charged in solution. During pyrrole′s electrochemical oligomerization mechanism, the existence of two cationic species is accepted, the radical cation generated by the oxidation process of neutral oligomers and the σ-dimer dication obtained after the radical−radical coupling. To elucidate which of the species corresponds to the observed dimer, the electrogenerated compounds were characterized by spectroscopic techniques.

Spectroscopic Characterization of the Electrogenerated Compounds (ESR and UV−vis). The suspicion of having an organic salt at the end of electrolysis and the possibility of observing radical species led us to use electron spin resonance spectroscopy (ESR). The *ex situ* analysis of the electrolyzed solution showed the presence of a stable radical after the Py-GSATA oxidation (Figure 5). The ESR signal fits with the

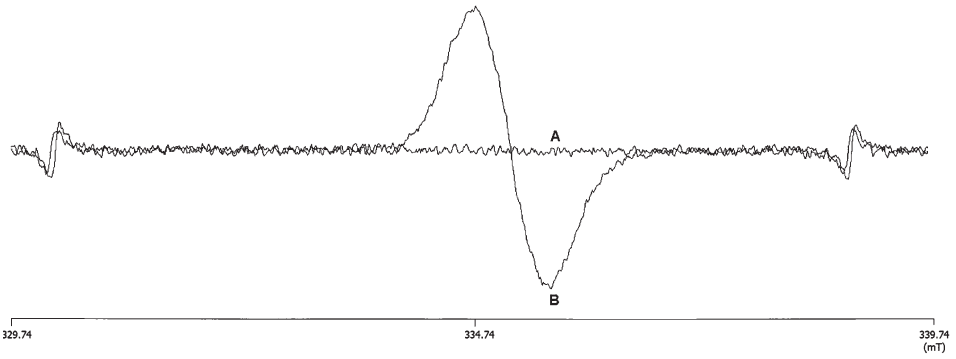

FIGURE 5. ESR spectra of (A) solution containing 0.1 M TBAP in ACN and 20 mM Py-GSATA (corresponds to Figure 5a) and (B) same solution analyzed after total electrolysis at 1.35 V vs Fc/Fc^+ (2.3 F/mol; corresponds to Figure 5c). Lateral ESR signals correspond to the internal standard MnO.

characteristics of an organic radical centered on 335.184 mT with hyperfine coupling value 2.0026. After electrogenerating the radical, it can be observed by ESR spectroscopy without substantial diminishing of the signal, if it is kept at 4 °C, for at least 6 months and for a month at room temperature. This result was unexpected because electrogenerated radical cation species are extremely reactive and are not easily detected. This is in agreement with the analysis of these solutions by cyclic voltammetry, where the peak at −0.35 V (signal IIc) is the sole signal present, and its current value also maintained its original value as long as the radical was ESR detected. Low temperature ESR and cyclic voltammetry (see below) experiments were carried out to get insight about the system. The ESR hyperfine radical couplings could not be better resolved under these experimental conditions. This is in agreement with recent reports about ESR studies of cation radicals of polyaromatic compounds, dimeric heterocycles,[23] and polypyrroles[24] where the depicted ESR spectra did not describe any hyperfine coupling. The spin concentration of the paramagnetic compound was determined using TEMPO as external marker yielding, after a 1:50 dilution, a spin concentration in the electrochemical cell of 9.35 mM (Figure S8 in Supporting Information). This value is very close to the expected 10 mM that should be present at the end of the electrolysis if the dimeric species is considered as the final compound. This confirms that the electrolysis solution contains the paramagnetic compound as major specie.

The Py-GSATA solution during electrolysis showed no precipitates, but an intense change of color passing from transparent (max abs 210 nm) to green-brownish dark was observed, which is characteristic of the formation of soluble oligomers.[25] In order to know the wavelength absorption of the stable radical oligomer and to compare it with other compounds described in literature, UV−vis spectroelectrochemistry was carried out in situ during the electrolysis process. In Figure 6, the spectra of the initial (Figure 6, a) and final (Figure 6, b) electrolysis solutions reveal the appearance of absorption bands located at 252, 275, 331,

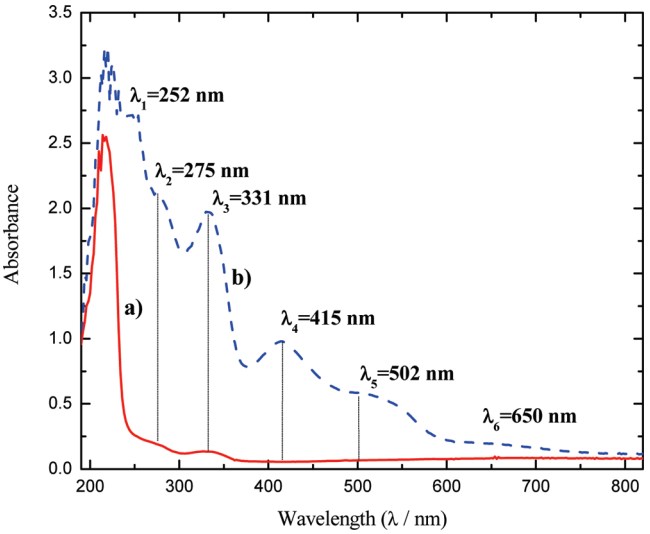

FIGURE 6. Initial (a) and final (b) UV−vis of the electrolysis at 1.42 V vs Fc/Fc^+ of a solution containing 0.1 M TBAP in ACN and 10 mM Py-GSATA. Cell volume 2 mL, using a Pt mesh as working electrode and in a separated compartment a copper mesh.

415, 502, and 650 nm. The change in absorbance, recorded every 30 s during the first minutes of the electrolysis (Figure S4 in Supporting Information), demonstrates that the first absorption bands to appear correspond to 252, 331, and 415 nm. The literature indicates that these peaks correspond to the presence of neutral pyrrole dimers, in our case to GSATA-Py-Py-GSATA.[2b,26] The peaks located at higher wavelengths (502 and 650 nm), which appeared at the end of the electrolysis, should correspond to the radical cation of this dimeric species (*vide infra*). An absorption peak at higher wavelengths was never observed, which is in agreement with the absence of long chain oligomers.

On the basis of the experimental results it is proposed that the product of the electrolysis responsible for voltammetric peak IIc corresponds to the dimer (2,2′)-GSATA-Py-Py-GSATA radical cation that arises from the decomposition of intermediate σ-dimer, observed as the peak Ic in voltammetry only in very special conditions (Figure 2 and Figure S1 in Supporting Information). To verify the stability of the

(23) (a) Rapta, P.; Schulte, N.; Schluter, A. D.; Dunsch, L. *Chem.—Eur. J.* **2006**, *12*, 3103–3113. (b) Song, C.; Swager, T. M. *Org. Lett.* **2008**, *10*, 3575–3578.

(24) Hsu, C. F.; Zhang, L.; Peng, H.; Travas-Sejdic, J.; Kilmartin, P. A. *Synth. Met.* **2008**, *158*, 946–952.

(25) Diaz, A. F.; Castillo, J.; Kanazawa, K. K.; Logan, J. A.; Salmon, M.; Fajardo, O. *J. Electroanal. Chem.* **1982**, *133*, 233–239.

(26) Serac, S.; Sonmez, G. *Polym. Int.* **2002**, *51*, 594–600.

TABLE 1. Theoretical Data in Solution (ACN) at the B3LYP/6-31+G Level of Theory for Some of the Species Generated during the Dimerization Process**

specie[a]	HOMO (eV)	LUMO (eV)	HOMO−LUMO gap (eV)	Gibbs free energy (kcal/mol)
M	−6.173	−0.649	5.523	−898 179.830
$M^{\bullet+}$	−8.055	−5.559	2.496	−898 043.703
D^{2+} σ-dimer	−8.128	−4.419	3.708	−1 796 081.600
D	−5.526	−0.779	4.746	−1 795 588.419
$D^{\bullet+}$	−6.810	−5.0153	1.795	−1 795 479.059
ClO_4^-				−83 554.966
$HClO_4$				−477 497.633
H^+				889

[a]M = monomer Py-GSATA ; D = dimer (2,2′)-GSATA-Py-Py-GSATA.

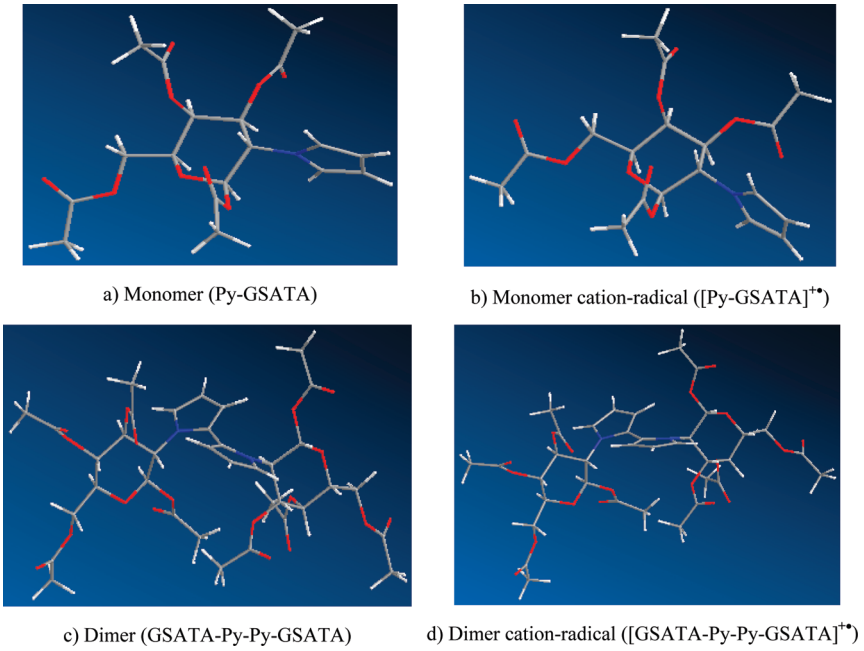

FIGURE 7. Optimized geometry of the Py-GSATA intermediates at B3LYP/6-31+G** level of theory. Dimer σ-dimer ([GSATA-(H)Py-Py(H)-GSATA]$^{++}$) and tetramer are depicted in Supporting Information (Figure S5).

intermediates generated during electrolysis, the oligomerization process was analyzed by means of a molecular modeling study. This led us to explain the presence of the dimeric species observed during the study.

Molecular Modeling of the Oligomerization Process of Py-GSATA and Stability of the Intermediates. To gain insight on the stability of the proposed species and to understand why the polymerization process did not occur, a theoretical study of the process was carried out. The structures of the neutral and charged species involved in the oligomerization process of the monomer Py-GSATA (monomer, σ-dimer, dimer, and tetramer) were optimized using B3LYP/6-31+G** level of theory in solution (ACN). The calculated species were chosen from the accepted mechanism of electropolymerization of pyrrole.[2] As previously shown,[27] when charged species are involved in electrochemical processes, the calculations should be carried out in solution to get reliable theoretical information. Vibration frequency calculations in solution were carried out to obtain the Gibbs free energy value ($H_{total} - TS$) for each species to determine the feasibility of the dimerization of Py-GSATA in solution via the thermochemical analysis shown in Scheme 1.

When the term adiabatic ionization is used, the geometrical and electronic relaxation of molecular systems with n and $n - 1$ electrons is taken into account, where the adiabatic ionization potential is the energetic difference between these two molecular species. In the present study, the Gibbs free energies calculated in solution resulted in the estimation of adiabatic ionizations (when indicated) since there is no significant change in either zero point energies or entropy from one species to another. Gibbs free, HOMO, and LUMO energies and the gap energy between these energies are shown in Table 1.

From Scheme 1, the dimer formation process energy (sum of coupling and regeneration of aromaticity reactions; second and third lines of Scheme 1) has a global ΔG value of 2.331 kcal, which denotes a barely favored process (approximately 20% of product might be present, according to the equation $K_{eq} = e^{-\Delta G/RT}$). This result reflects the difficulty of coupling between two monomeric radical cation species, presumably due to the steric hindrance exerted by the bulky acetate groups near the pyrrole rings.

In Figure 7, it can be observed that as the oligomerization process moves forward monomer → dimer → tetramer, the sterical hindrance around the pyrroles chain becomes more important as a result of the increment in the number of

(27) Osorio, G.; Frontana, C.; Frontana-Uribe, B. A.; Guadarrama, P. *J. Phys. Org. Chem.* **2004**, *17*, 439–447.

acetate groups, placing the pyrrole rings out of the plane with the consequent break of conjugation. The twisted conformation of the hypothetical tetramer (for tetramer optimized geometry see Figure S5 in Supporting Information) would limit the aromaticity of the backbone, restraining in this way the stability of higher oligomers.

To confirm that the spin density distribution of the dimer radical cation does not limit the oligomerization process, it was calculated at the UB3LYP/6-31+G** level of theory (Figure S6 in Supporting Information). In this representation, it is clearly observed that the majority of the spin distribution (red color) on $D^{\bullet+}$ is located on positions 2, 3, and 5, where the polymerizations should take place. Thus, the lack of polymerization cannot be attributed to electronic factors. An important factor that should limit the formation of higher oligomers is the sterical hindrance of the acetate groups during the process. In the Py-GSATA monomer crystal structure,[15] in the neutral (Figure 7a) and the radical-cation species (Figure 7b), the pyrrole group shows a conformation perpendicular to the sugar plane as a response to the bulky acetate groups. When the dication σ-dimer is formed, the sterical hindrance of acetate groups on pyrrole groups is extremely high. The loss of two protons to make the neutral dimer does not result in a favorable situation to facilitate the next coupling reactions. The continuation of the oligomerization process requires coupling of electrogenerated radical cations at 2 or 5 pyrrole positions, but at this stage the pyrroles' approach is extremely limited by the cloud of acetate groups that surround the bipyrrole group in the dimer cation-radical (Figure 7d).

The HOMO−LUMO gap value (Table 1) of the monomer (5.523 eV, 224 nm) corresponds with the absorption value observed at $\lambda = 210$ nm in the UV−vis spectrum registered before electrolysis (Figure 6a). The smallest gap value was found for the dimer cation radical (1.795 eV, 690 nm), which is consistent with the absorption observed at $\lambda = 650$ nm obtained from the electrolyzed solution (Figure 6, b). There is also a clear relationship between the HOMO−LUMO gap and the electron delocalization of different species involved in the dimerization process. As expected, going from monomer to dimer, the gap gets closer and denotes the corresponding expansion of the electronic delocalization due to a better orbital overlapping. Around the same Δ of 0.7 eV, the $M \rightarrow D$ and $M^{\bullet+} \rightarrow D^{\bullet+}$ steps are preserved. The high stability of the dimer radical cation species is in agreement with the favorable electronic delocalization associated with the small HOMO−LUMO gap of this molecule. There is a Δ of almost 3 eV, going from $D^{\bullet+}$ to D, related to the loss of electronic delocalization with the concomitant loss of stability. These results are in agreement with the optimized geometry of the intermediates, where it can be seen that the bipyrrole backbone has a better coplanarity in the dimer radical-cation species than in the neutral dimer (Figure 7d vs Figure 7c).

On the other hand, the bulky acetate groups that prevent oligomerization seem to be responsible as well for the remarkable stability of the dimer radical cation species, exerting a protecting effect.[6] The effective protection of the radical cation species by the bulky acetate groups that surround the bipyrrole group in the cation-radical generates a "seashell-like" structure (Figure 7d). This sterical protection effect of the radical center by hindered groups has been observed previously for other stable radicals and radical cations.[6,7,28,29] Nevertheless, other possible sources of stabilization, for example, the direct participation of the acetate groups to generate a covalent bond, cannot be discarded at this stage. Thus, both the avoidance of the oligomerization and the amazing stability of the dimer radical cation in solution can be explained by two reasons: the higher coplanarity observed for the dimer radical-cation structure, a sign of efficient charge delocalization on the system, which is not observed in the neutral dimer; and the second and probably the most important, the sterical protection effect of the cloud of acetate groups or/and the chemical participation of these groups to generate a new highly stabilized structure of $D^{\bullet+}$.

Low Temperature Electrochemical Behavior of the $D^{\bullet+}$. The electrolyzed solution containing the stable paramagnetic species was analyzed at different lower temperatures (Figure S7 in Supporting Information). It was observed that peak IIc, obtained at the end of the electrolysis, changes its shape as the temperature decreases, from a peak with some indicators of reversibility (Figure S7a in Supporting Information) to a typical irreversible peak with five small reversible signals after the main cathodic process (Figure S7d in Supporting Information). This result suggests a change in the reactivity of the electrogenerated $D^{+\bullet}$ with temperature. When the temperature is decreased, the first system clearly defined is that of the highest negative potential. As the temperature reached −28 °C, systems with less cathodic potential started to be defined; this behavior is classic from electroactive oligomers with different sizes of chain.[8] Voltamperograms suggest that at low temperature the dimeric radical cation is consumed by an oligomerization process to yield the longer chain products detected by the cyclic voltammetry experiments at higher cathodic potential (Figure S7d in Supporting Information). Even so, a deposit of polymer on the electrode was not obtained; probably the polymerization does not occur and only very soluble higher oligomers are obtained in low concentration under these conditions. This change of reactivity of the dimeric radical cation with the temperature, observed in the cyclic voltammetry, can be attributed to a change of the acetate groups' rotation speed. At room temperature, the fast rotation of these groups provokes an umbrella effect that prevents the pyrrole radical coupling and protects the radical species, but this effect should be minimized by lowering the temperature, and the spin density located at positions 2 and 5 (Figure S6 in Supporting Information) should favor the oligomerization process.

Conclusion

The electrochemical characterization by cyclic voltammetry of Py-GSATA showed two irreversible oxidation signals: the first at 1.24 and the second at 1.54 V vs Fc^{+}/Fc. It is not possible to electropolymerize this pyrrole derivative to generate a chiral conducting polymer. Using ESR and UV−vis

(28) (a) Hicks, R. G. *Org. Biomol. Chem.* **2007**, *5*, 1321–1338. (b) Power, P. P. *Chem. Rev.* **2003**, *103*, 789–809.

(29) Altwicker, E. R. *Chem. Rev.* **1967**, *67*, 475–531.

(30) Heinze, J.; Rasche, A.; Pagels, M.; Geschke, B. *J. Phys. Chem. B* **2007**, *111*, 989–997.

(31) Zhao, Y.; Schultz, N. E.; Truhlar, D. G. *J. Chem. Theory Comput.* **2006**, *2*, 364–382.

(32) Selvi, S.; Pu, S.; Cheng, Y.; Fang, J.; Chou, P. *J. Org. Chem.* **2004**, *69*, 6674–6678.

spectroscopy, a persistent cation-radical dimer was characterized as the main product of the electrooxidation of Py-GSATA. Molecular modeling of the oligomerization intermediates using the B3LYP/6-31+G** level of theory showed that cooperative stability factors operate to limit the oligomerization process and to stabilize the dimer cation radical. A reaction mechanism that explains the observed behavior, based on the thermochemical computed data, is proposed.

Experimental Section

Substances, Solvent, and Supporting Electrolyte. 1,3,4,6-Tetra-*O*-acetyl-2-(pyrro-1-yl)-2-deoxy-β-D-glucopyranose (Py-GSATA) (Figure 1) was prepared as described in the literature.[15] Anhydrous acetonitrile (CH_3CN, ACN) was used as received, handling the sealed bottle under positive N_2 pressure. Tetrabutylammonium perchlorate (Bu_4NClO_4, TBAP, electrochemical grade) was used as supporting electrolyte. The salt was dried the night before its use at 90 °C, and 0.1 M solutions were prepared and used as the supporting electrolyte.

Electrodes, Apparatus, and Instrumentation. Cyclic voltammetry was performed with a potentiostat/galvanostat. A conventional three-electrode cell was used to carry out these experiments, employing as working electrode a platinum microelectrode (BAS MF-2013, 1.6 mm dia), polished using 0.05 μm alumina, sonicated in distilled water for 5 min, and acetone-rinsed prior to its use. A platinum mesh was used as counter-electrode (surface, 0.6 cm^2). The experimental potential values were obtained using the Ag/Ag^+ reference electrode (BAS MF-2062 Ag/0.01 M $AgNO_3$ 0.1 M TBAP in ACN), separated from the medium by a Vycor membrane. The graphed and reported E_p values are versus the ferricinium/ferrocene couple (Fc^+/Fc), according to the IUPAC recommendation.[16] The potential of the Fc^+/Fc couple against the Ag/Ag^+ reference electrode was 0.10 V. Solutions of Py-GSATA were prepared by dissolving this compound with 0.1 M TBAP at a concentration range of 1−10 mM. The solution was deoxygenated for 10−15 min, and the cell was kept under a nitrogen atmosphere (grade 5, ultrapure) throughout the experiment. Preparative electrolyses were performed using a potentiostat-galvanostat and a digital coulombimeter. For these experiments, a two-compartment electrochemical cell separated by a sintered glass (pore No. 4) was used. Working and reference (in anodic chamber) and counter electrode (in cathodic chamber) consisting of platinum meshes (3.25 cm^2) were fitted inside the cell. The Ag/Ag^+ reference electrode was introduced into the anodic compartment. The two chambers were filled with 25 mL of previously deoxygenated (N_2, 30 min) supporting electrolyte. Py-GSATA (198.7 mg, 0.5 mmol) was added to the anolyte and dissolved by stirring magnetically under a N_2 flux. The electrolyses were carried out potentiostatically at a working potential of 1.35 V vs Fc/Fc^+. Evolution of the reaction was followed by cyclic voltammetry and by thin layer chromatography. Mass spectroscopy was carried out using FAB^+ technique.

ESR and UV−vis Spectroscopy Experiments. ESR spectra were recorded in the X band (9.85 GHz) using an spectrometer with a cylindrical cavity, and all spectra were calibrated using as internal reference MnO (G: 2.0330, H: 330.162, and G: 1.9810, H: 338.856). All spectra were obtained in ACN solution at different temperatures. The spin concentration of the paramagnetic compound was determined using 2,2,6,6-tetramethyl-1-piperidin-1-oxo (TEMPO) compound as external marker; the electrolysis solution was diluted (1:50) with pure anhydrous ACN containing the supporting electrolyte and the ESR spectra were taken at different electrolysis times. A diode array spectrophotometer was used for the spectroelectrochemical experiments, with a thin spectrometric cell (2 mL) equipped with a divided (Vycor) three-electrode system: a platinum mesh as working electrode and Ag/AgBr as reference electrode, both located in the anodic compartment, and a copper mesh in the cathodic chamber. For the potential imposition, a computer-controlled potentiostat/galvanostat was used with the software provided by the manufacturer. Exhaustive electrolyses of solutions of Py-GSATA (1−20 mM) were carried out for these experiments. The UV−vis spectra were recorded for 30 and 60 s, depending on the electrolyses duration.

Theoretical Methodology. All initial structures were constructed with Chem3D Ultra package (version 10.0) [1986−2006 Cambridge Soft Corporation]. DFT framework was used in the present study. Full geometry optimization calculations in solution (ACN; dielectric constant $\varepsilon = 38$) were carried out at the B3LYP/6-31+G** level of theory. The unrestricted shell formalism was used when open shell systems were calculated. Solvation was calculated using the self-consistent reaction field method with its own Poisson−Boltzmann solver,[17] which represents the solvent as a layer of charges at the molecular surface, providing in this way a dielectric continuum boundary. The hybrid functional B3LYP (Becke and Lee−Yang−Parr)[18] was chosen because of its very good performance in geometrical predictions of common organic molecules, showing errors less than 0.005 Å on average for bond lengths.[19] Gibbs free energies were calculated at the same level of theory (B3LYP/6-31+G**) by single point frequency calculations of the previously optimized geometries. Both the functional and the split valence basis set 6-31+G** (including polarized and diffuse functions) are included in the program Jaguar v.7.0 (Schrodinger, LLC, New York, NY, 2007).

Acknowledgment. The authors kindly thank Virginia Gomez, Luis Velasco, and Francisco Javier Perez for their technical assistance. U.P.-G. thanks CONACyT-Mexico for a postdoctoral scholarship. Part of the research was carried out with funds from CONACyT-Mexico, project No 57856.

Supporting Information Available: Experimental details, atom coordinates and absolute energies of calculated structures, figures mentioned in the article. This material is available free of charge via the Internet at http://pubs.acs.org.